# A new approach to multi-robot harbour patrolling: theory and experiments

Alessandro Marino, Gianluca Antonelli, A. Pedro Aguiar, António Pascoal

*Abstract*— **This paper describes a decentralized coordination strategy for multi robot patrolling missions. To this effect, the theory of Gaussian Processes (usually used for estimation purposes) is suitably adapted to tackle the problem of harbour patrolling. The introduction of a time varying dependency in the probabilistic formulation (thus allowing for the sampled field to be dynamic, i.e., changing in time) makes the proposed solution suitable for the type of mission considered. Moreover, the advantages of Voronoi tessellations are exploited to automatically distribute the vehicles over the environment. The resulting algorithm takes into account several constraints and can be tailored based on the communication and computational capabilities of the robots, thus making it suitable for heterogeneous systems. Numerical simulations and experiments involving three autonomous marine surface vehicles in a harbour scenario at the Parque Expo site in Lisbon are discussed.**

## I. Introduction

Among the multitude of tasks requiring the use of multi-robot systems, the following are worth stressing; environmental exploration and sampling, terrain coverage, air and ocean monitoring, and patrolling. Examples of these tasks can be found in [5], [19], [13]. These tasks have one key factor in common: they require that the robots be dynamically positioned so as to meet some optimality criterion in the presence of specific, application-related constraints.

In particular, the problem of sampling amounts to devising a strategy to move a group of sensors in the environment and have them visit a number of locations so as to maximize the amount of information available to characterize a given phenomenon. Stated in more detail, in the case of a scalar field (eg., salinity, temperature, etc.), the objective for the mobile robots is to carry the sensors to locations that better (according to some metric) allow for the prediction of the value of the field even in points where no direct measurements are made in such a way as to reduce the global prediction uncertainty.

To formally study this problem, an appealing mathematical tool emerges out of the theory of Gaussian processes [17] mostly used for sampling fields that allows for the prediction of the values of a physical variable at spatial points of interest and, at the same time, to compute the uncertainty involved in that prediction [14]. This methodology can be extended to deal with dynamical fields, the evolution of which depends explicitly on time as shown, for example, in [8]. In this case, the vehicles in charge of mapping the field may have to revisit previously sampled locations in order to capture the time-varying characteristics of the phenomenon of interest.

The above framework, developed with sampling applications in mind, yields naturally in this paper a methodology for patrolling in 2D or 3D environments. In fact, the framework adopted allows us to address in an elegant fashion the concept of sensor range of the vehicles and the frequency at which a given location should be visited. Furthermore, in real scenarios, some locations require to be visited at higher frequency (e.g., the entrance of an harbour) and a suitable solution for this requirement is naturally provided with the methodology adopted.

Because we will be dealing with multi-robot systems in order to obtain decentralized architectures, in the problem formulation one must explicitly address the constraint that each vehicle will only communicate with neighbour vehicles. See for example [15] for interesting work along these lines. In this work, mobile sensors move on structured tracks that have been optimized over a minimal set of parameters based on a given metrics in order to sample a given field. In addition, practical issues were also addressed. Groundbreaking work on ocean sampling is described in [16], where autonomous vehicles carrying environmental sensors are coordinated in order to efficiently sample the ocean.

In this paper, the main objective is the study of the patrolling problem. The strategy adopted exploits recent results in [8], is distributed and optimal according to a well defined criteria, and takes explicitly into account the communication capabilities of the robots.

In the work presented, use is made of the properties of Voronoi tessellations which effectively endow the vehicles with the capability to automatically spread themselves over the environment according to a defined criteria. See [12], [9] or [11] for examples of recent application of Voronoi tessellations mainly related to the coverage problem. With this set-up, each vehicle builds its only partition of the area to be covered in reaction to the perceived position of the neighbour vehicles without requiring access to the state of the entire team of vehicles. The proposed approach was also tested on a real setup with three marine surface vehicle. Good performance has been observed, together with robustness and consequently applicability of the algorithm in real applications in the presence of external disturbances (e.g., ocean currents) and faults in the communications.

The paper is organized as follows. Section II describes briefly the key mathematical tools and background results exploited in this work. Section III introduces the patrolling

A. Marino is with the University of Salerno, Via Ponte don Melillo, 84084, Salerno (SA), Italy almarino@unisa.it

G. Antonelli is with the Dipartimento di Ingegneria Elettrica e dell'Informazione, Università di Cassino e del Lazio Meridinoale, Via G. Di Biasio 43, 03043, Cassino (FR), Italy, antonelli@unicas.it.

António Pascoal and A. Pedro Aguiar are with the ISR/IST - Institute for Systems and Robotics, Instituto Superior Técnico, Torre Norte 8, Av. Rovisco Pais, 1049-001 Lisbon, Portugal, {antonio,pedro}@isr.ist.utl.pt.

strategy, including implementation aspects. Finally, Section IV contains the results of simulation and experimental results. As stated above, the latter were obtained in the course of an actual mission motivated by a harbour patrolling scenario. To this effect, three Medusa autonomous surface vehicles designed and assembled by the robotic team of the IST/ISR (Instituto Superior Técnico/Institute for Systems and Robotics) were operated simultaneously to perform a one-hour patrolling mission at the Parque EXPO site in Lisbon.

## II. Mathematical Background

This section summarizes some background material and the main mathematical tools adopted in this paper. In particular, brief descriptions of Gaussian Processes and of Voronoi tessellations are provided.

### A. The Gaussian Processes

Gaussian Processes have been widely used to sample fields modeled as stochastic phenomenons [17]. An important problem that has been studied in the past and is currently receiving new interest from a practical point of view, especially in marine scenarios, is the task of estimating the spatial distribution of a scalar field over a region of interest. In oceanographic application the variable of interest might be the temperature or salinity distribution over the domain space [14].

To this aim, Gaussian modeling is an appealing tool given its interesting properties. A Gaussian process can be defined as a collection of a finite number of random variables, where each one is characterized by a joint Gaussian distribution. In the sequel we will consider random processes of the form

$$f(\boldsymbol{x}, t) = \mu(\boldsymbol{x}, t) + \zeta(\boldsymbol{x}, t), \tag{1}$$

where $\boldsymbol{x} \in \mathbb{R}^l$ ($l = 2, 3$) denotes the position of a point in the 2D or 3D domain, $\mu$ is the mean of the process at position $\boldsymbol{x}$ and time $t$, which is supposed to be known, and $\zeta$ is a second-order stationary random process with zero mean and known covariance function $\mathcal{K}$.

We will assume that the covariance function $\mathcal{K}$ is generically defined as

$$\begin{aligned} \mathcal{K}(f_1, f_2) &= \mathcal{K}(f(\boldsymbol{x}_1, t_1), f(\boldsymbol{x}_2, t_2)) \\ &= C(\|\boldsymbol{x}_2 - \boldsymbol{x}_1\|, |t_2 - t_1|) \end{aligned} \tag{2}$$

with $C : \mathbb{R}_0^+ \times \mathbb{R}_0^+ \to \mathbb{R}^+$. It is important to stress that the spatio-temporal process $f$ depends both on the location $\boldsymbol{x}$ and time $t$ in order to explicitly take into account also the case of time-varying scalar fields. Furthermore, eq. (2) implicitly assumes that the process is homogeneous, second order stationary and isotropic, which basically implies that the covariance only depends on the distance between two generic points $\boldsymbol{x}_1$ and $\boldsymbol{x}_2$ and on the absolute value of the time difference $t_2 - t_1$. Clearly, other models can be used that takes into account anisotropic sensor models.

In the following, given a set of points and instants of time $S = \{(\boldsymbol{x}_1, t_1), (\boldsymbol{x}_2, t_2), \ldots, (\boldsymbol{x}_n, t_n)\}$, the symbol $\Sigma_S \in \mathbb{R}^{n \times n}$ represents the symmetric non-negative covariance matrix whose elements $(i, j)$ is $\mathcal{K}(f_i, f_j)$.

Moreover, given a single element $(\boldsymbol{x}, t)$, $\boldsymbol{\Sigma}_{Sx} \in \mathbb{R}^n$ is a column vector whose $i$-th element is $\mathcal{K}(f(\boldsymbol{x}, t), f(\boldsymbol{x}_i, t_i))$.

In the case of a multivariate normal distribution over a set $S$ of random variables associated at $n$ pairs of position, instants of time, the joint probability distribution is given by

$$p(\boldsymbol{f}) = \frac{(2\pi)^{-n/2}}{|\boldsymbol{\Sigma}_S|^{1/2}} e^{-\frac{1}{2}(\boldsymbol{f} - \boldsymbol{\mu}_S)^T \boldsymbol{\Sigma}_S^{-1} (\boldsymbol{f} - \boldsymbol{\mu}_S)} \tag{3}$$

where:

$$\boldsymbol{f} = \begin{bmatrix} f_1 & f_2 & \cdots & f_n \end{bmatrix}^{\mathrm{T}} \in \mathbb{R}^n$$

is the vector of the random variables at the given elements of the set $S$,

$$\boldsymbol{\mu}_S = \begin{bmatrix} \mu(\boldsymbol{x}_1, t_1) & \mu(\boldsymbol{x}_2, t_2) & \cdots & \mu(\boldsymbol{x}_n, t_n) \end{bmatrix}^{\mathrm{T}} \in \mathbb{R}^n$$

is the corresponding column vector of means, and $\boldsymbol{\Sigma}_S \in \mathbb{R}^{n \times n}$ is the covariance matrix.

### B. Inferring the information from the acquired samples

One of the advantages of using Gaussian processes is that marginalization is not complex. Consider again the set $S$, where each element $(\boldsymbol{x}_i, t_i)$ contains the position and the instant of time that sample $y_i$ of the scalar field represented by eq. (1) has been measured.

Let $\boldsymbol{y} = \begin{bmatrix} y_1 & y_2 & \ldots & y_n \end{bmatrix}^{\mathrm{T}}$ be the column vector of the acquired samples.

Given a single element $(\boldsymbol{x}, t)$, we denote by $p(\hat{y}|\boldsymbol{y})$ the distribution of the predicted measurement $\hat{y}$ of $f(\boldsymbol{x}, t)$ given the acquired samples.

It is possible to demonstrate that for multivariate Gaussian processes this conditional distribution is still a Gaussian distribution with the following synthetic representation [17]:

$$\hat{\mu} = \mu(\boldsymbol{x}, t) + \boldsymbol{\Sigma}_{Sx}(\boldsymbol{x}, t)^{\mathrm{T}} \boldsymbol{\Sigma}_S^{-1} (\boldsymbol{y} - \boldsymbol{\mu}) \tag{4a}$$

$$\hat{\Sigma} = \mathcal{K}(f(\boldsymbol{x}, t), f(\boldsymbol{x}, t)) - \boldsymbol{\Sigma}_{Sx}(\boldsymbol{x}, t)^{\mathrm{T}} \boldsymbol{\Sigma}_S^{-1} \boldsymbol{\Sigma}_{Sx}(\boldsymbol{x}, t) \tag{4b}$$

where:

- $\hat{\mu} \in \mathbb{R}$ is the predicted mean given the acquired samples (mean of the posterior probability);
- $\boldsymbol{y} = \begin{bmatrix} y_1 & y_2 & \cdots & y_n \end{bmatrix}^{\mathrm{T}} \in \mathbb{R}^n$ is the column vector collecting the acquired samples of the scalar field of the random variables at the point of the set $S$;
- $\boldsymbol{\mu} = \begin{bmatrix} \mu(\boldsymbol{x}_1, t_1) & \mu(\boldsymbol{x}_2, t_2) & \cdots & \mu(\boldsymbol{x}_n, t_n) \end{bmatrix}^{\mathrm{T}} \in \mathbb{R}^n$ is the column vector collecting the means of the random variables at point of the set $S$;
- $\boldsymbol{\Sigma}_{Sx}$ is a column vector representing the covariance matrix between $f(\boldsymbol{x}, t)$ and the random variables at the points in the set $S$;
- $\boldsymbol{\Sigma}_S \in \mathbb{R}^{n \times n}$ is the covariance matrix relative to random variables at the points in set $S$.

In the above, the matrices $\boldsymbol{\Sigma}_S$ and $\boldsymbol{\Sigma}_{Sx}$ are completely defined once the function $C$ in eq. (2) has been specified.

According to [17] and [20], one possible choice for this function is the Square Exponential Covariance Function:

$$C(\|\boldsymbol{x}_2 - \boldsymbol{x}_1\|, |t_2 - t_1|) = \phi^2 e^{-\frac{\|\boldsymbol{x}_2 - \boldsymbol{x}_1\|^2}{2\tau_s^2} - \frac{(t_2 - t_1)^2}{2\tau_t^2}}, \quad (5)$$

where $\phi$ is a weighting scalar parameter that will be selected to be unitary and the parameter $\tau_s$ and $\tau_t$ are positive scalars used to affect the space and time scales, respectively; the latter need to be properly designed [20]. In addition, it is worth noticing that the choice in eq. (5) refers to isotropic domains and known constant $\tau_s$ and $\tau_t$. The case of adaptive parameter estimation as also been addressed in the literature; see for example [18] and the references therein.

Matrix $\boldsymbol{\Sigma}_S(\boldsymbol{x}, t)$, is the covariance between a measurement taken at $\boldsymbol{x}_i$ at $t_i$ and one at an unknown location $\boldsymbol{x}$ at time $t$. The meaning of eq. (5) is intuitive: the more the samples are spatially and temporally distant the more they are independent.

### C. Application to the patrolling mission

From eq. (4b), the covariance of the conditional distribution at a position $\boldsymbol{x}$ and current time $t$ takes the form

$$\hat{\Sigma}(\boldsymbol{x}) = C(0, 0) - \boldsymbol{\Sigma}_{Sx}{}^{\mathrm{T}} \boldsymbol{\Sigma}_S^{-1} \boldsymbol{\Sigma}_{Sx}. \quad (6)$$

From eq. (4b) it turns out that minimizing the uncertainty, which corresponds to minimizing the positive definite right-hand side of eq. (6), is the same as maximizing (given the available degrees of freedom) the function

$$\xi(\boldsymbol{x}) = \boldsymbol{\Sigma}_{Sx}{}^{\mathrm{T}} \boldsymbol{\Sigma}_S^{-1} \boldsymbol{\Sigma}_{Sx}. \quad (7)$$

Note also that due to the time dependency of the covariance function in (5), a point that has been visited too far in the past (with respect to the time parameter $\tau_t$) is candidate to be visited again. This feature makes the approach suitable for the patrolling task as explained in the next section, but it can also be exploited for other tasks like sampling.

The function in eq. (7) has several features that can be inherited by a the patrolling algorithm. In detail:

- the parameter $\tau_s$ in (5) can be used to model the visibility range of the on board sensors (as intruder detection sensors). Note that eq. (5) also models the growing uncertainty of the sensor readings with the distance from the sensor. In addition, by setting $\tau_s$ as a function of the position $\boldsymbol{x}$, we can take into account that the visibility range of vehicles' sensors could depend on the environment (operating conditions);
- the parameter $\tau_t$ in (5) can be used to model the desired frequency visit of the various locations. In fact, lower values of this parameter causes the function in eq. (7) to decrease faster with time thus making more uncertain the corresponding points;
- by setting $\tau_t = \infty$ in eq. (5) a static field is obtained. This feature could be used to perform a coverage mission;
- the parameter $\tau_t$ in eq. (5) might be a function of the location $\boldsymbol{x}$. By setting this parameter lower in some locations with respect to others, it is possible to increase the frequency of visits in sensible locations;
- the function in eq. (7) can be used for 2D and 3D environment.

### D. The Voronoi partition

The Voronoi tessellation has been used as a useful tool to achieve coordination among robots. It allows for a partition of the domain to patrol in a distributed manner. The Voronoi partitions (or diagrams) are subdivisions of a set $\mathcal{D}$ characterized by a metric with respect to a finite number of points belonging to the set.

Let $\boldsymbol{x}$ be a generic point of $\mathbb{R}^l$, $l = 2, 3$. The $i$-th robot position is denoted as $\boldsymbol{x}_{r,i} \in \mathbb{R}^l$. The vector $\boldsymbol{x}_r \in \mathbb{R}^{ln}$ collects the positions of all the $n$ robots.

Given a set or robots' positions $\{\boldsymbol{x}_{r,1}, \boldsymbol{x}_{r,2}, \ldots, \boldsymbol{x}_{r,n}\}$ with $\boldsymbol{x}_{r,i} \in \mathbb{R}^l$, the corresponding $n$ Voronoi cells, $Vor(\boldsymbol{x}_{r,i})$, are given by

$$Vor(\boldsymbol{x}_{r,i}) = \{\boldsymbol{x} \in \mathcal{D} \quad | \quad \|\boldsymbol{x} - \boldsymbol{x}_{r,i}\| \leq \|\boldsymbol{x} - \boldsymbol{x}_{r,j}\|, \forall j\}.$$

It is interesting to highlight that the computation of the Voronoi cells is structurally distributed: each robot at point $\boldsymbol{x}_{r,i}$ can compute the corresponding cell $Vor(\boldsymbol{x}_{r,i})$ by simply knowing its position and the *neighbors*' positions.

## III. Proposed coordination strategy

Several aspects and constraints might affect the execution of a patrolling mission, e.g., occurrence of robot faults, large number of patrolling robots, limited communication range and computational capabilities. For these reasons, the following aspects need to be investigated:

- *Distribution*. The control architecture needs to be fully distributed.
- *Communication*. The vehicles should be able to communicate. In particular, it is considered that each vehicle can exchange information only with its neighbors as will be clear in the following sections.
- *Collision avoidance*. It is obvious to require that each patrolling robot must avoid collisions with other teammates or obstacles, even in the case of a large number of robots.
- *Experimental validation*. Because of the practical interest of the patrolling mission, an important feature of the desired strategy is that it must be implementable in a real setup.

The architecture of the proposed scheme is depicted in Figure 1. The architecture shown refers to the single robot. At the top level, there is the robot's planner that is in charge of deciding the robot motion commands. This level will be described in Section III-A. At the middle level, the Null-Space-based-Behavioral (NSB) control allows to properly handle eventually conflicting tasks. The NSB has been widely used in the past. The interested reader can find in [6], [7], the details of this strategy and its properties. In this paper, it is used only to allow the robot to reach the desired goal while avoiding eventually present obstacles. Finally, the lower level comprises the computing hardware/software and

the mechanical features of the single robot; the structure of this layer depends on the robotic platform being used and is primarily concerned with the available sensors and actuators. The setup used in this work is detailed in Section IV.

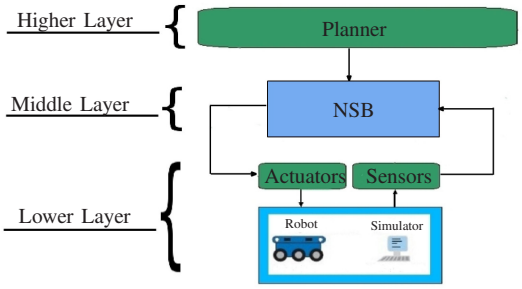


Fig. 1. Sketch of the control architecture.

### A. The top level: algorithm description

In this section, the motion commands generation for the vehicles are described.

At the core of the algorithm is the non-linear function $\xi(\boldsymbol{x})$ expressed in eq. (7). Several approaches may be considered as, for example, maximization of its integral or maximization of its minimum, depending on the specific application.

To enforce a distributed algorithm, each robot computes locally the next via point to visit in the corresponding Voronoi cell in order to decrease the amount of uncovered area. To this effect, whenever possible each robot exchanges information with neighbours to compute the Voronoi partition and to maintain an estimate of the function $\xi(\boldsymbol{x})$ that depends on the state of the whole system [8]. Details about the required information exchange are provided in the Section III-B. The use of the Voronoi tessellation is particularly useful because it also allows to avoid conflicts among the vehicles.

The strategy designed for each robot is the following:

**Algorithm 1** Harbor patrolling.

**loop**
1) build $Vor(\boldsymbol{x}_{r,i})$ based on local information
2) request updating data to local neighbors
3) properly choose inside its own partition the next point $\overline{\boldsymbol{x}}_i$ to reach, based on the function $\xi(\boldsymbol{x})$
4) command the robot toward the point $\overline{\boldsymbol{x}}_i$ while avoiding obstacles
**end loop**

With regards to step 1, it has been assumed that each vehicle is capable of estimating the position of its neighbours (in the Delaunay sense). It is worth noticing that this hypothesis could not be verified in large environments or short-range vehicles. Representative work in this direction is described in by [10]. Regarding step 3, the following strategy is implemented by each vehicle for the choice of the next point $\overline{\boldsymbol{x}}_i$ to visit. Each robot choices the next point to visit inside its own Voronoi partition $Vor(\boldsymbol{x}_{r,i})$. Inside $Vor(\boldsymbol{x}_{r,i})$, the most uncertain points are represented by the lowest values of the function $\xi(\boldsymbol{x})$. Because $\boldsymbol{\Sigma}_S$ a symmetric positive matrix, the lower bound of the quadratic form $\xi(\boldsymbol{x})$ is obviously 0. Notice also from (4b) that its upper bound is $\phi^2$. This means that, being $\phi = 1$, $\xi(\boldsymbol{x})$ is upper-bounded by 1. A proper threshold, $\theta$, in the range $[0,\ 1]$ can be chosen and the set $S_u(\theta)$ considered: $S_u(\theta) = \{\boldsymbol{x}_u \in Vor(\boldsymbol{x}_{r,i}) \mid \xi(\boldsymbol{x}_u) < \theta\}$. Among the points belonging to $S_u$ the next point to visit is chosen according to some criteria (for example, furthest point from the actual vehicle position, the point characterized by the lowest value of the function $\xi$, etc.). In this work, we propose the following strategy. Let $\boldsymbol{x} = \boldsymbol{f}(s)$ be a parametrization of the segment joining the actual position $\boldsymbol{x}_{r,i}$ of the vehicle and a generic point $\boldsymbol{x}_u \in S_u$, being $s \in [0,\ 1]$ the curvilinear abscissa; the point in $S_u$ that minimizes the index

$$\frac{\int_0^1 \xi(\boldsymbol{f}(s))ds}{\|\boldsymbol{x}_{r,i} - \boldsymbol{x}_u\|} \tag{8}$$

is chosen as the next target. The heuristics behind the strategy (8) is that, among the unvisited points in the set $S_u$, the one characterized by the most unvisited path (normalized by the path length) is chosen.

### B. Implementation issues

The strategy described in Algorithm (1) requires each robot to calculate the function $\xi(\boldsymbol{x})$ only inside its own Voronoi partition. Nevertheless, the knowledge of the set $S$ that contains the samples acquired by all the robots in the different locations and at different time instants is still needed. In [8], it is explained how each robot could estimate $\xi(\boldsymbol{x})$ in its Voroni partition by information exchange.

## IV. Simulation and Experiments

### A. Simulation results

Numerical simulations were performed in order to illustrate the performance of the proposed algorithm. In the simulations, three vehicles cooperated in a patrolling mission at a maximum speed of 3 km/h. Different videos were created to clearly show some important features of the proposes approach:

- Video [3] shows the movements of the vehicles in the case of a static field, i.e. $\tau_t = \infty$ and $\tau_s = 0.3\,\text{Km}$ in eq. (5);
- Video [2] shows the movements of the vehicles in the case of a dynamic field with $\tau_t = 0.5\,\text{h}$ and $\tau_s = 0.3\,\text{Km}$;
- Video [1] shows the movements of vehicles in the case of a dynamic field with $\tau_s = 0.3\,\text{Km}$ but $\tau_t$ is configuration dependent. In particular, the time constant $\tau_t$ that sets the decay rate of the function (7) is smaller in the sea region further away from the coast to simulate the fact that intruders might come from the open sea; as a consequence, the vehicles should patrol that region more frequently.

A dynamic obstacle is present moving randomly in the environment.

Four approaches to the problem of cooperative patrolling were tested for comparison purposes. In the simulation set-up, 3 vehicles evolve across a field characterized by $\tau_t = 0.9\,\text{h}$, $\tau_s = 0.2\,\text{km}$. A dynamic obstacle moves randomly in the region of operation, a square with side length equal to $4\,\text{km}$. The approaches considered are listed below.

- *The lawnmower approach*. The environment is divided in three equal rectangular slices. Inside each slice the vehicle moves repeatedly up and down as an automatic lawn mower would do.
- *The approach proposed in this paper*.
- *The random approach*. The vehicles moves randomly in the field without any communication
- *The deployment approach*. The vehicles are coordinated according to the algorithm described in [9] with the density function in eq. (7).

Figure 2 shows the integral of the function $\xi(\boldsymbol{x})$ over the domain of operation, as function of time. Notice that the deployment approach causes the vehicles to reach a static configuration, yielding large amount of the region unexplored. The random approach gives, obviously, better performance than the deployment approach, but worse than the lawn mower-like approach where the vehicles' paths causes the performance index to increase but also to oscillate. This is in striking contrast with the superior performance obtained with the approach proposed in this paper, as Figure 2 clearly shows.

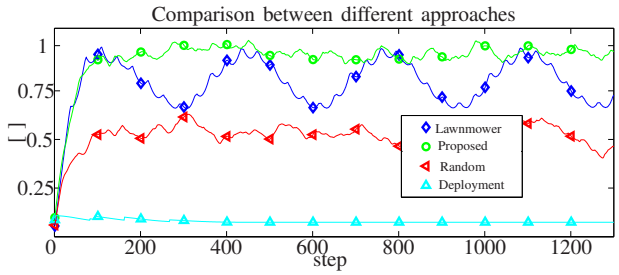


Fig. 2. Normalized Performance index for the lawnmower-type motion (blue), proposed approach (green), random motion (red) and deployment (cyan).

## B. Experiments

Experiments were done with the three autonomous surface vehicles shown in Figure 3 (red, black, and yellow vehicles).

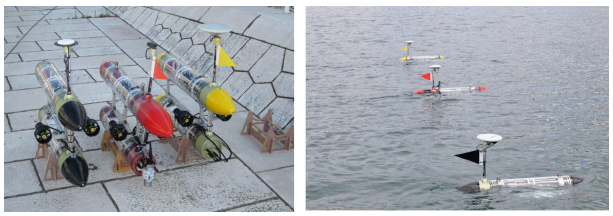

Fig. 3. The three Medusa surface vehicles setup (the red, black and yellow vehicles).

Each vehicle, named Medusa, was entirely designed and assembled by the staff of the Dynamical Systems and Ocean Robotics Laboratory (DSOR-Lab) of the ISR/IST of Lisbon. They consist of two identical bodies, an upper body and a lower body with diameters and lengths of $0.15\,\text{m}$ and $1\,\text{m}$, respectively. The distance between the two bodies is $0.45\,\text{m}$. The lower underwater body contains a lithium polymer battery pack together with the actuator electronics. The upper part contains the processing unit together with navigation sensors (mainly, IMU and GPS). For control, navigation, and mission control systems implementation, each vehicle runs a standard Linux operative system on a 2 GHz Intel Core Duo-1 GB RAM platform. The architecture adopted allows for seamless implementation and hardware-in-the-loop testing of solutions developed in the MatLab environment. The vehicles are equipped with a GPS localization system. Inter-vehicle and vehicle/underwater target communications are enabled via Wi-Fi and acoustic modem networks, respectively. At the nominal speed of $1.0\,\text{m/s}$, the vehicles have an autonomy of $6\,\text{hours}$. The autonomy can be doubled by adding an extra battery pack. The maximum rated speed of the vehicles is $2.0\,\text{m/s}$. At the moment no sensor is mounted on the vehicle to detect intruders in an harbour patrolling scenario: the uncertainty map is updated based only on the vehicles' positions.

The experiments were run in the Summer of 2011 at the Parque Expo site, Lisbon, Portugal. A video of the experiments can be found in [4]. Figure 4 shows the map of the site, with the robots moving in a $60\,\text{m}\times 70\,\text{m}$ rectangular map. An obstacle consisting of a buoy is placed inside the patrolling region (the green dot in Figure. 4). The position of the buoy is fixed and known in advance by the vehicles. The maximum vehicles speed was limited to $0.7\,\text{m/s}$. In what follows we summarize the results of an experiment that run for approximately 1 hour.

The vehicles exchanged information via WI-FI network. The $\tau_s$ and $\tau_t$ parameters were set to $3.7\,\text{m}$ and $200\,\text{s}$, respectively; the constant $\theta$ in Section III-A was set to $0.2$.

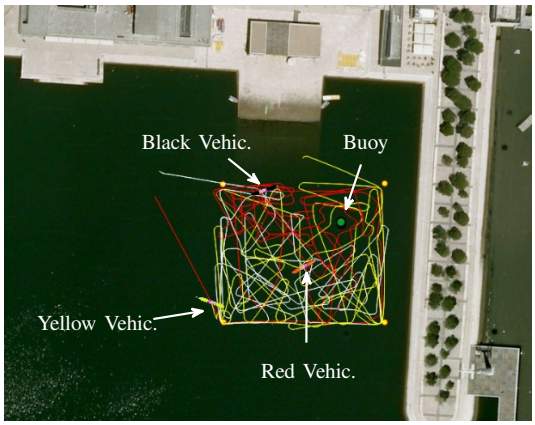


Fig. 4. The map of the Parque Expo site in Lisbon with the paths described by the vehicles in a typical experiment. The vehicles (red, black and yellow) are restricted to move in a $60\,\text{m}\times 70\,\text{m}$ rectangular environment.

In Figure 5, the sequence of steps performed by the vehicles is shown. In each frame, on the left are shown the Voronoi cells with the vehicles and the current targets (big bullets) while, on the right, the plot of function (7) is shown. The red color is representative of higher values of

the function while the blue color of lower ones. Focusing the attention on the black vehicle, the following steps are shown:

1) the vehicle moves toward the current target as generated by the algorithm described in Section III,
2) the vehicle reaches the current target,
3) the vehicle chooses the next target inside its own Voronoi cell,
4) the vehicle moves toward the new target.

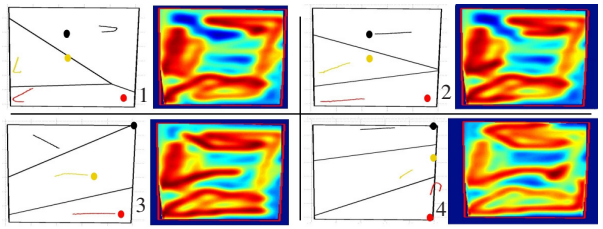


Fig. 5. Frames of the experiments. In each frame, on the left are shown the Voronoi cells with the vehicles and the current targets (big bullets) while, on the right, the plot function $\xi(\boldsymbol{x})$ in eq. (7) is shown (red color is representative of high values of the function, blue color of low values). Frame#1. The black vehicle is approaching the corresponding target. Frame#2. The black vehicle has approached the target. Frame#3. After the black vehicle has reached the target, the next one is generated inside its own cell. Frame#4. The black vehicle moves toward the new target.

Finally, in Figure 6 the integral of the function in $\xi(\boldsymbol{x})$ normalized to the maximum value obtained over the environment is plotted with respect to time. Notice how the function almost reaches a steady value as confirmed by the simulations in Section IV-A.

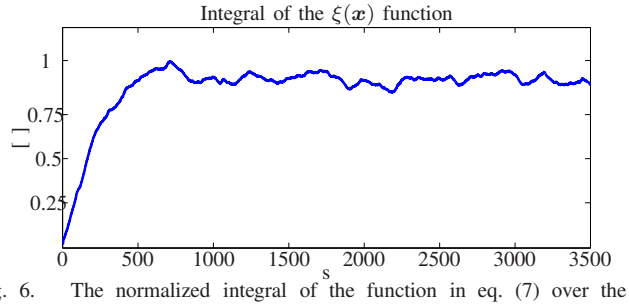


Fig. 6. The normalized integral of the function in eq. (7) over the environment.

## V. Conclusions

A distributed approach for multi-robot patrolling was proposed. The strategy adopted exploits a probabilistic framework to define the vehicle's motion strategy.

Based on Voronoi tessellation techniques, each vehicle chooses the next point to reach inside its Voronoi cell in order to reduce the unexplored locations. As an added value with respect to related work, experiments were run using three autonomous marine vehicles available at the ISR/IST of Lisbon. As future work, the case of one or more intruder vehicle entering the patrolled area will be considered. In addition, also the case of limited range communications will be addressed explicitly.

## Acknowledgments

The research leading to these results has received funding from the European Community's Seventh Framework Programme under grant agreement n. 231378 (STREP project Co$^3$AUVs) and under the Italian Government under grant FIRB n. RBFR08QWUV (NECTAR) and PRIN 2008 n. 2008EPKCHX (MEMONET).

Our special thanks go to the technical staff of the Dynamical Systems and Ocean Robotics Laboratory (DSOR-Lab) of the ISR/IST of Lisbon for their unvaluable support in making the MEDUSA vehicles available for tests.

## References

[1] *http://webuser.unicas.it/lai/robotica/video/SimNotUniformDynamicField.avi*.
[2] *http://webuser.unicas.it/lai/robotica/video/SimDynamicField.avi*.
[3] *http://webuser.unicas.it/lai/robotica/video/SimStaticField.avi*.
[4] *http://webuser.unicas.it/lai/robotica/video/VideoLisbonExpo.avi*.
[5] A. Almeida, G. Ramalho, H. Santana, P. Tedesco, T. Menezes, , and V. Corruble. Recent advances on multi-agent patrolling. *Proceedings of the Brazilian Symposium on Artificial Intelligence*, 2004.
[6] G. Antonelli. Stability analysis for prioritized closed-loop inverse kinematic algorithms for redundant robotic systems. *IEEE Transactions on Robotics*, 25(5):985–994, 2009.
[7] G. Antonelli, F. Arrichiello, and S. Chiaverini. The Null-Space-based Behavioral control for autonomous robotic systems. *Journal of Intelligent Service Robotics*, 1(1):27–39, January 2008.
[8] G. Antonelli, A. Marino, and S. Chiaverini. A coordination strategy for multi-robot sampling of dynamic fields. In *Proceedings International Conference on Robotics and Automation*, St. Paul, Minnesota, USA, May, 14-18, 2012, (accepted).
[9] F. Bullo, J. Cortés, and S. Martinez. *Distributed Control of Robotic Networks*. Princeton University Press, 2008.
[10] J. Cortes, S. Martinez, and F. Bullo. Spatially-distributed coverage optimization and control with limited-range interactions. *ESAIM: Control, Optimisation and Calculus of Variations*, 2005.
[11] J. Cortes, S. Martinez, T. Karatas, and F. Bullo. Coverage control for mobile sensing networks. *IEEE Transactions on Robotics and Automation*, 20(2):243–255, 2004.
[12] Q. Du, V. Faber, and M. Gunzburger. Centroidal Voronoi tessellations: applications and algorithms. *SIAM review*, 41(4):637–676, 1999.
[13] A. García-Olaya, F. Py, J. Das, and K. Rajan. An online utility-based approach for sampling dynamic ocean fields. *IEEE Journal ofOceanic Engineering*, (2):185–203, 2012.
[14] A. Krause, C. Guestrin, A. Gupta, and J. Kleinberg. Near-optimal sensor placements: maximizing information while minimizing communication cost. In *IPSN 06*, Nashville, Tennessee, USA, April, 19-21 2006.
[15] N.E. Leonard, D. A. Paley, F. Lekien, R. Sepulchre, D.M. Fratantoni, and R.E. Davis. Collective Motion, Sensor Networks, and Ocean Sampling. *Proceedings of the IEEE*, 95(1):48–74, January 2007.
[16] N.E. Leonard, D.A. Paley, R.E. Davis, D.M. Fratantoni, F. Lekien, and F. Zhang. Coordinated control of an underwater glider fleet in an adaptive ocean sampling field experiment in monterey bay. *Journal of Field Robotics*, 27(6):718–740, 2010.
[17] C. E. Rasmussen and C. Williams. *Gaussian processes for machine learning*. MIT Press, 2006.
[18] A. Singh, A. Krause, C. Guestrin, W. Kaiser, and M. Batalin. Efficient planning of informative paths for multiple robots. In *In Porecedeengs of 20th International Joint Conference on Artifical Intelligence*, San Francisco, CA, USA, 2007.
[19] R. Smith, J. Das, H. Heidarsson, A. Pereira, F. Arrichiello, I. Cetinic, L. Darjany, M. Garneau, M. Howard, C. Oberg, M. Ragan, E. Seubert, E. Smith, B. Stauffer, A. Schnetzerand G. Toro-Farmer, D. Caron, B. Jones, and G. Sukhatme. The USC center for integrated networked aquatic platforms (CINAPS): Observing and monitoring the southern California bight. *accepted for publication IEEE Robotics and Automation Magazine, Special Issue on Marine Robotic Systems*, 17(1):20–30, 2010.
[20] Y. Xu and J. Choi. Mobile sensor networks for learning anisotropic gaussian processes. In *American Control Conference*, St. Louis, MO, USA, June, 10-12 2009.